Highly Selective DNA Alkylation at the 5′ Side G of a 5′GG3′ Sequence by an Aglycon Model of Pluramycin Antibiotics through Preferential Intercalation into the GG Step

Kazuhiko Nakatani,* Akimitsu Okamoto, Takahiro Matsuno, and Isao Saito*

Contribution from the Department of Synthetic Chemistry and Biological Chemistry, Faculty of Engineering, Kyoto University, and CREST, Japan Science and Technology Corporation, Kyoto 606-8501, Japan

Received March 10, 1998

Abstract: Altromycin B and kapurimycin A_3 are new members of the pluramycin family antibiotics that alkylate N7 of guanine (G) in duplex DNA at an epoxide subunit attached to the C2 position of the pyranone ring. While 5′AG3′ selective alkylation by altromycin B was accounted for by selective binding to the sequence, it remained uncertain why kapurimycin A_3, which is structurally similar to an aglycon part of altromycin B but has an epoxide subunit with an opposite absolute configuration, selectively alkylates 5′ G of the 5′GG3′ sequence. To clarify the molecular basis for the sequence-selective G alkylation by kapurimycin A_3, we have examined the DNA cleavage sequence selectivity of an enantiomeric pair of an aglycon model of pluramycin antibiotics and calculated total energy change upon intercalation of the model into a specific sequence by means of the DFT-HF hybrid method at the B3LYP/6-31G(d) level. Only an enantiomer with the same epoxide absolute configuration as that of kapurimycin A_3 showed a remarkable G alkylation reactivity with a high selectivity for 5′ G of the 5′GG3′ sequence. Molecular mechanics calculations suggested that the intercalation of the aglycon model in an orientation perpendicular to neighboring base pairs is essential for the effective G alkylation at 5′ G of GN sequences, and the efficiency for G alkylation is not dependent upon the sequence being intercalated. DFT-HF hybrid calculations suggested that the intercalation of the model is energetically most favorable into GG step. These results suggested that highly 5′ G selective alkylation of the GG sequence by kapurimycin A_3 arises from a selective intercalation into the GG step. Stacking interaction with both 5′ and 3′ side Gs is a basis for the stabilization of the intercalated complex.

Introduction

Altromycin B (**1**)[1,2] and kapurimycin A_3 (**2**)[3,4] are new members of the pluramycin family antibiotics[5] and alkylate N7 of guanine (G) in duplex DNA at an epoxide subunit attached to the C2 position of the pyranone ring.[6−10] NMR studies on the DNA adduct of **1** have shown that the antibiotic intercalates into the DNA duplex at the 5′ side of the alkylated G in an orientation perpendicular to neighboring base pairs.[11,12] The

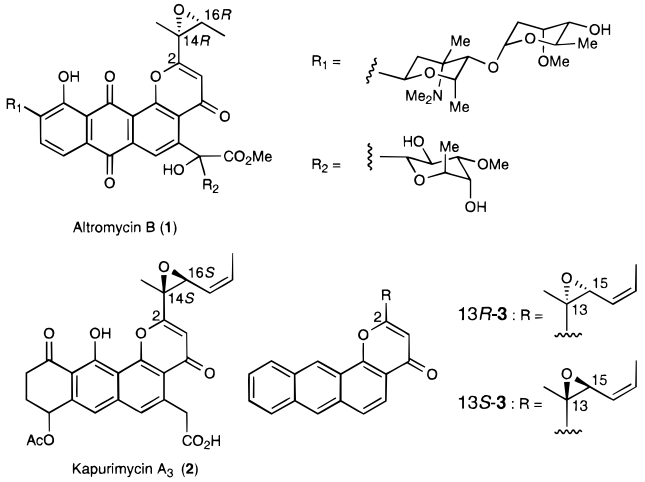

observed 5′AG*3′ selectivity (* denotes the alkylated site) for the G alkylation by **1** was accounted for by a preferential binding to this sequence through a DNA−sugar interaction.[8,11] In contrast, preferential alkylation of 5′ G of the 5′GG3′ sequence was observed with **2**,[10,13] which is structurally similar to an aglycon part of **1** but has an alkenyl epoxide subunit with an opposite absolute configuration (14*S*, 16*S*).[14] Since there is no

* Corresponding author: (phone) (+81)-75-753-5656; (fax) (+81)-75-753-5676; (e-mail) saito@sbchem.kyoto-u.ac.jp.

(1) Jackson, M.; Karwowski, J. P.; Theriault, R. J.; Hardy, D. J.; Swanson, S. J.; Barlow, G. J.; Tillis, P. M.; McAlpine, J. B. *J. Antibiot.* **1990**, *43*, 223−228.

(2) Brill, G.; McAlpine, J. B.; Whittern, D. N.; Buko, A. M. *J. Antibiot.* **1990**, *43*, 229−237.

(3) Hara, M.; Mokudai, T.; Kobayashi, E.; Gomi, K.; Nakano, H. *J. Antibiot.* **1990**, *43*, 1513−1518.

(4) Yoshida, M.; Hara, M.; Saitoh, Y.; Sano, H. *J. Antibiot.* **1990**, *43*, 1519−1523.

(5) Séquin, U. *Fortschr. Chem. Org. Naturst.* **1986**, *50*, 57−122.

(6) Sun. D.; Hansen, M.; Clement, J. J.; Hurely, L. H. *Biochemistry* **1993**, *32*, 8068−8074.

(7) Hansen, M.; Yun, S.; Hurley, L. H. *Chem. Biol.* **1995**, *2*, 229−240.

(8) Hansen, M. R.; Hurley, L. H. *Acc. Chem. Res.* **1996**, *29*, 249−258.

(9) Hara, M.; Yoshida, M.; Nakano, H. *Biochemistry* **1990**, *29*, 10449−10455.

(10) Chan, K. L.; Sugiyama, H.; Saito, I. *Tetrahedron Lett.* **1991**, *52*, 7719−7722.

(11) Hansen, M.; Hurley, L. H. *J. Am. Chem. Soc.* **1995**, *117*, 2421−2429.

(12) Sun, D.; Hansen, M.; Hurley, L. H. *J. Am. Chem. Soc.* **1995**, *117*, 2430−2440.

(13) Nakatani, K.; Okamoto, A.; Saito, I. *Angew. Chem. Int. Ed. Engl.* **1997**, *36*, 2794−2797.

(14) Uosaki, Y.; Saito, H. 69th annual meeting of the Chemical Society of Japan, Kyoto, 1995; Abstr. p 1013.

10.1021/ja980801q CCC: $15.00
Published on Web 10/21/1998

Scheme 1

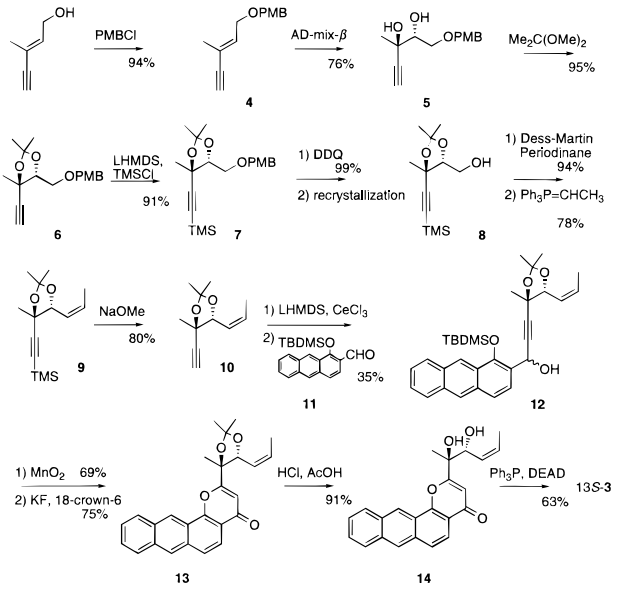

Scheme 2

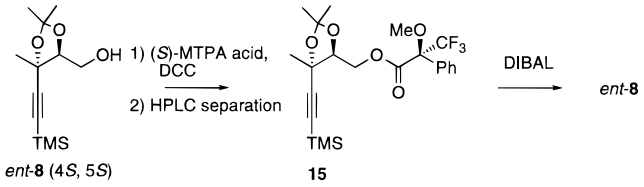

apparent structural determinant for **2** to bind selectively to the 5′GG3′ sequence, the molecular basis for the 5′G*G3′ selectivity has remained uncertain. To clarify this point, we have carried out comparative G alkylation experiments using an enantiomeric pair of a simplified aglycon model of pluramycins and calculated the total energy change upon intercalation of this model into a specific DNA sequence by means of the DFT-HF hybrid method at the B3LYP/6-31G(d) level. On the basis of these theoretical and experimental results, it was demonstrated that the highly GG selective alkylation observed for **2** is derived from an intrinsic property of the GG step in B-form duplex DNA, which stabilizes the intercalated complex much more strongly than any other G-containing sequences do by stacking interaction with both 5′ and 3′ side Gs.

Results and Discussion

Synthesis of Aglycon Models. To assess the effect of structure on the sequence selectivity, we have investigated G alkylation by aglycon models 13*R*-**3** and 13*S*-**3** bearing an alkenyl epoxide subunit of absolute configurations exactly corresponded to **1** and **2**, respectively. Both 13*R*-**3** and 13*S*-**3** isomers were synthesized via a synthetic route to that similar to that reported earlier (Scheme 1).[13,15,16] Since the enantiomeric purity of **5** obtained by asymmetric dihydroxylation of **4** with AD-mix-β was not high (about 80% ee), alcohol **8** was recrystallized to obtain enantiomerically pure (4*R*,5*R*)-**8** ($[\alpha]^{25}_{D}$ = +19.34, c = 0.610, MeOH). In the synthesis of the enantiomer of **8** (*ent*-**8**), HPLC separation of a diastereomeric mixture of (*S*)-MTPA ester **15** followed by reductive deacylation provided enantiomerically pure *ent*-**8** ($[\alpha]^{25}_{D}$ = −19.17, c = 0.120, MeOH) (Scheme 2). Oxidation of **8** was followed by

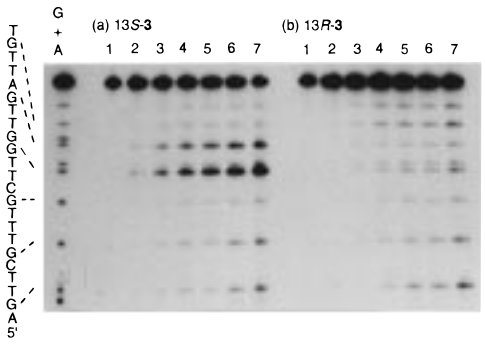

Figure 1. Cleavage of 43-mer ODN via G alkylation by (a) 13*S*-**3** and (b) 13*R*-**3**. ^{32}P 5′-end-labeled ODN was annealed with a complementary strand and incubated with drug (50 μM) in Tris-HCl (pH 7.6) at 37 °C for the period indicated. ODN was recovered by ethanol precipitation, heated at 90 °C for 30 min with 10% piperidine, and analyzed on 15% denatured PAGE. Lanes: 1, control; 2, 1 h; 3, 3 h; 4, 5 h; 5, 7 h; 6, 10 h; 7, 24 h; G + A, Maxam−Gilbert G + A lane. A partial sequence of ODN is shown in the left.

Wittig olefination to produce **9** (Z:E = ∼10:1), which was desilylated to give alkyne **10**. Lithiated **10** was coupled with 1-(*tert*-butyldimethylsilyloxy)-2-anthraldehyde (**11**) to give adduct **12**. Oxidation followed by pyranone ring cyclization[15,16] efficiently produced tetracyclic compound **13**, which was finally transformed after deprotection to 13*S*-**3** by intramolecular Mitsunobu reaction.

Analysis of G Alkylation Sequence Selectivity for Aglycon Models. Sequence selectivities of 13*R*-**3** and 13*S*-**3** were investigated using a 43-mer oligodeoxynucleotide (ODN), d(TTTTTGTT*TG*TT*AG*TT*CG*TTT*GC*TT*GG*TT*GA*TT*GT*TTG-TTTTT), having all seven possible G-containing sequences (italic). The ^{32}P 5′-end-labeled ODN was annealed with a complementary strand, and the duplex was incubated with 13*R*-**3** and 13*S*-**3**. Alkylated G sites were detected as cleavage bands after hot piperidine treatment by means of denatured polyacrylamide gel electrophoresis (PAGE). As is clear from Figure 1, 13*R*-**3** having an epoxide group with the same absolute configuration as **1** showed only weak and equal G bands (Figure 1b, lanes 4−7). In sharp contrast, strong and highly selective G bands were observed with 13*S*-**3** preferentially at 5′ G of the 5′GG3′ sequence and to a lesser extent at the GA sequence (Figure 1a, lanes 4−7). The alkylation susceptibility of GN sequences (N = A, C, G, T) decreased in the order of 5′GG3′ > GA ≫ GT > GC, and the normalized relative G band intensities (I_{G*N}) for G*G, G*A, G*T, and G*C as obtained by densitometric analysis of lane 4 (Figure 1a) were 64.3, 26.6, 5.7, and 3.4, respectively. A large difference in both reactivity and sequence selectivity between these enantiomers is particularly noteworthy.[17] Efficient and highly sequence selective alkylation at 5′ G of the 5′GG3′ by 13*S*-**3** possessing the same epoxide absolute configuration as **2** provided strong evidence that such 5′ G selective alkylation proceeds via a DNA−drug complex which can be produced only from a 13*S* isomer.

Simulation of Intercalated Complex of 13*S*-3 into DNA. The 5′G*G3′ alkylation selectivity observed for **2** may arise

(15) Nakatani, K.; Okamoto, A.; Yamanuki, M.; Saito, I. *J. Org. Chem.* **1994**, *59*, 4360−4361.

(16) Nakatani, K.; Okamoto, A.; Saito, I. *Tetrahedron* **1996**, *52*, 9427−9446.

(17) For recent examples of different DNA alkylation properties of drug enantiomers, see: (a) Boger, D. L.; McKie, J. A.; Nishi, T.; Ogiku, T. *J. Am. Chem. Soc.* **1997**, *119*, 311−325. (b) Patel, V. F.; Andis, S. L.; Enkema, J. K.; Johnson, D. A.; Kennedy, J. H.; Mohamadi, F.; Schultz, R. M.; Soose, D. J.; Spees, M. M. *J. Org. Chem.* **1997**, *62*, 8868−8874. (c) Borger, D. L.; Yun, W. *J. Am. Chem. Soc.* **1994**, *116*, 7996−8006. (d) Boger, D. L.; Johnson, D. S.; Yun, W. *J. Am. Chem. Soc.* **1994**, *116*, 1635−1656. (e) Kigoshi, H.; Imamura, Y.; Mizuta, K.; Niwa, H.; Yamada, K. *J. Am. Chem. Soc.* **1993**, *115*, 3056−3065. (f) Boger, D. L.; Yun, W.; Terashima, S. Fukuda, Y.; Nakatani, K.; Kitos, P.; Jin, Q. *Bioorg. Med. Chem. Lett.* **1992**, *2*, 759−765.

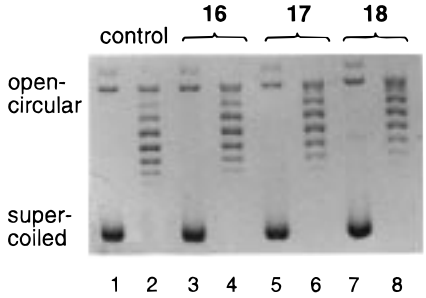

Figure 2. Unwinding of supercoiled pBR322 DNA by benzo-, naptho-, and anthrapyranone derivatives **16**−**18**, respectively. Supercoiled pBR322 DNA (250 ng) (lane 1) was first treated with topoisomerase l (topo l) (4 units) for 30 min at 37 °C in a buffer (10 mM Tris-HCl, pH 7.9, 1 mM EDTA, 150 mM NaCl, 0.1 mM spermidine, 5% glycerol, 0.1% BSA) and further incubated for 30 min in the absence (lane 2) and presence of **16**−**18** (100 μM) (lanes 4, 6, and 8, respectively). In lanes 3, 5, and 7, DNAs were incubated with **16**−**18**, respectively, in the absence of topo l. The resulting DNAs were analyzed by electrophoresis on 1% native agarose gel at 1.3 v/cm for 18 h. Lanes: 1, supercoiled DNA; 2, DNA treated with topo l; 3, **16**; 4, **16** plus topo l; 5, **17**; 6, **17** plus topo l; 7, **18**; 8, **18** plus topo l.

from a noncovalent binding step and/or a covalent alkylating step.[8] Previous structure−reactivity studies on truncated models of **2** showed that G alkylation reactivity increased with increasing ability for their intercalative binding.[13] DNA-unwinding assays with benzo-, naphtho-, and anthrapyranone derivatives **16**, **17**, and **18**, all of which lack an epoxide subunit

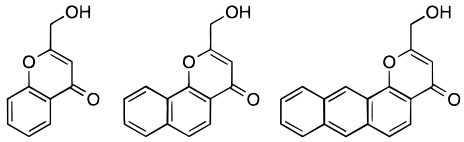

for DNA alkylation, were examined. The DNA-unwinding assay indicated that **18** intercalates into DNA much more strongly than **16** and **17** (Figure 2).

Molecular mechanics (MM) calculations of the intercalated complex of 13*S*-**3** into the GN/MC step, where M is a complementary base for N of duplex 6-mer d(ATGNTA/TAMCAT) were carried out by MacroModel (version 6.0) using the Amber* force field with GB/SA solvation treatment of water (distant-dependent dielectric electrostatic, cutoff for van der Waals, electrostatic, and hydrogen bonding were 8, 20, and 4 Å, respectively).[18] 13*S*-**3** was manually inserted into the GN/MC step of B-form duplex d(ATGNTA/TAMCAT) and the complexes were energy minimized to give initial geometries for molecular dynamics (MD) simulation. Stochastic dynamics simulation was carried out under the following conditions: initial temperature of 300 K, simulation temperature of 300 K, thermal bath time constant of 0.2 ps, simulation time step of 0.75 fs, and simulation length of 100 ps. These simulations indicated that the intercalation of 13*S*-**3** in an orientation perpendicular to neighboring base pairs is essential to steer the epoxide subunit proximal to the N7 of 5′ G with an appropriate alignment for the S_N2 epoxide ring-opening reaction (Figure 3). The average nonbonding distance between N7 of 5′ G and the epoxy carbon (C_{15}) and the angle for N7 of G, C_{15}, and the epoxy oxygen (O_3) are shown in Table 1 and are virtually the same for all complexes. These results suggested that the efficiency for G alkylation is insensitive to the sequence to be intercalated.[19] On the basis of these arguments, it was presumed that (i) the crucial step for 5′G*G3′ selectivity is a noncovalent binding step and (ii) the sequence selectivity for the G alkylation directly reflects the susceptibility for the intercalative binding of 13*S*-**3** to the GN/MC step.

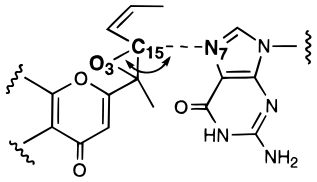

Energy Calculation of GN and GN·13*S*-3 Complex. To gain further insight into the relative stability of the complex formed by intercalation of 13*S*-**3** into the GN/MC step (GN·13*S*-**3**), total energy change upon intercalation was calculated by the DFT-HF hybrid method at the B3LYP/6-31G(d) level using the Gaussian 94 program.[20,21] Geometries of GN·13*S*-**3** and the two-base pair unit of GN/MC (GN) used for energy calculations were prepared as follows: for the GN·13*S*-**3** complex, 10 structures were sampled every 10 ps from MD simulation of the complex of 13*S*-**3** intercalated into the GN/MC step of the duplex 6-mer d(ATGNTA/TAMCAT). The structures were energy minimized and simplified for quantum calculations by removing two bases from both the 5′ and 3′ ends of the duplex 6-mer and the sugar phosphate backbone. A methyl group was attached to N9 and N1 of the purine and pyrimidine bases, respectively, instead of deoxyribose, giving the GN·13*S*-**3** structure. The structure of GN was made from the energy-minimized duplex by a similar procedure as described above. One of the 10 structures for each complex of GG·13*S*-**3**, GA·13*S*-**3**, GT·13*S*-**3**, and GC·13*S*-**3** used for energy calculation is shown in Figure 4. These coordinates of GN, 13*S*-**3**, and GN·13*S*-**3** were transformed into Gaussian input data by using Spartan (version 5.0). Single-point energy calculation of each GN, 13*S*-**3**, and GN·13*S*-**3** complex was carried out at the B3LYP/6-31G(d) level to give their total energies E_{GN}, $E_{13S\text{-}3}$, and $E_{GN\cdot 13S\text{-}3}$, respectively. $E_{GN\cdot 13S\text{-}3}$ was obtained as an average energy of 10 independent structures for each GN·13*S*-**3** (Table 2). The total energy change upon intercalation of 13*S*-**3** into the GN/MC step (ΔE_{GN}) and the relative energy difference of intercalation between the GN/MC and GG/CC steps ($\Delta\Delta E_{GN\text{-}GG}$) were obtained by eqs 1 and 2, respectively.

$$\Delta E_{GN} = E_{GN\cdot 13S\text{-}3} - E_{GN} - E_{13S\text{-}3} \quad (1)$$

$$\Delta\Delta E_{GN\text{-}GG} = \Delta E_{GN} - \Delta E_{GG} \quad (2)$$

Relative Intercalation Susceptibility into the GN/MC Step. Our calculations pointed out that the intercalative binding of 13*S*-**3** was energetically most favorable to the GG/CC step (Table 3). The order of GG > GA > GT > GC for the stability of the intercalated complex (i.e., ΔE_{GN}) is consistent with

(18) Still, W. C.; Tempczyk, A.; Hawley, R. C.; Hendrickson, T. *J. Am. Chem. Soc.* **1990**, *112*, 6127−6129.

(19) Average nonbonding distance between C_{15} of 13*R*-**3** and 3′ side G N7 in GG·13*R*-**3** complex obtained by MD simulation was 5.08 Å (0.52).

(20) Energy calculations at the B3LYP/6-31G(d) level with Gaussian 94 were carried out on a VPP300/16 supercomputer at the JST supercomputer complex.

(21) Gaussian 94, Revision D.4. Frisch, M. J.; Trucks, G. W.; Schlegel, H. B.; Gill, P. M. W.; Johnson, B. G.; Robb, M. A.; Cheeseman, J. R.; Keith, T.; Petersson, G. A.; Montgomery, J. A.; Raghavachari, K.; Al-Laham, M. A.; Zakrzewski, V. G.; Ortiz, J. V.; Foresman, J. B.; Cioslowski, J.; Stefanov, B. B.; Nanayakkara, A.; Challacombe, M. Peng, C. Y.; Ayala, P. Y.; Chen, W.; Wong, M. W.; Andres, J. L.; Replogle, E. S.; Gomperts, R.; Martin, R. L.; Fox, D. J.; Binkley, J. S.; Defrees, D. J.; Baker, J.; Stewart, J. P.; Head-Gordon, M.; Gonzalez, C.; Pople, J. A. Gaussian, Inc., Pittsburgh, PA, 1995.

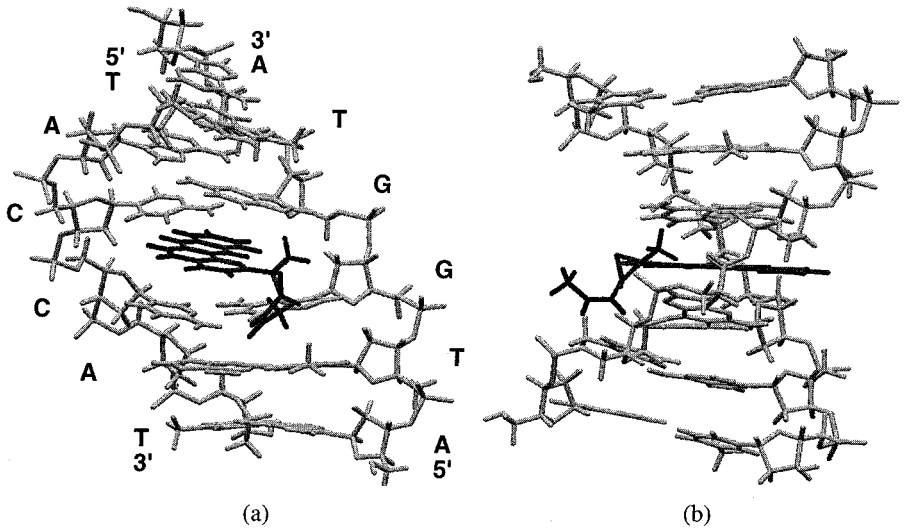

Figure 3. Energy-minimized structure of complex of d(ATGGTA/TACCAT) with 13*S*-**3**, in which 13*S*-**3** intercalated into the GG step. DNA and 13*S*-**3** are shown in gray and black, respectively. Views from (a) a major groove and (b) a direction parallel to GC base pairs.

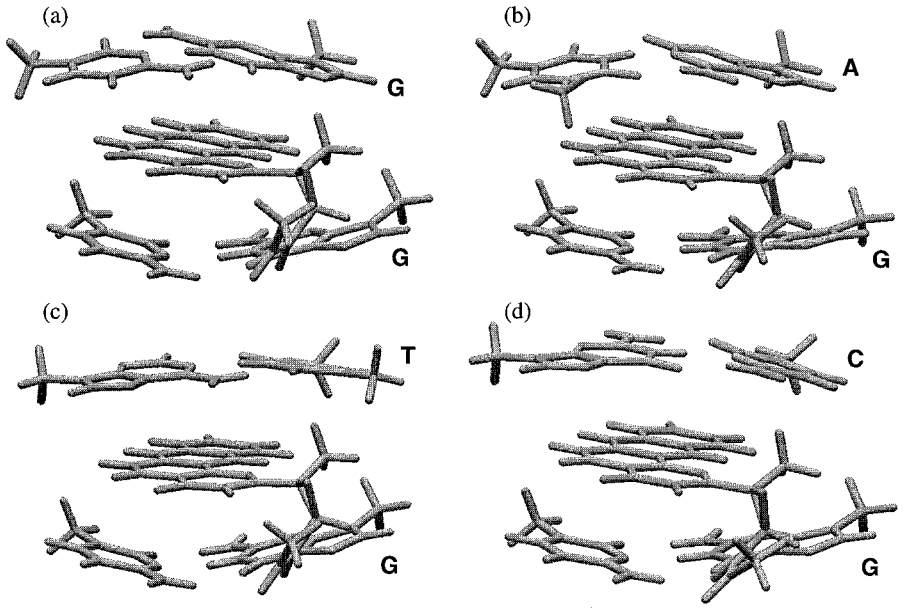

Figure 4. Representative structures of four 5′GN3′·13*S*-**3** complexes used for B3LYP/6-31G(d) energy calculations: (a) GG·13*S*-**3**; (b) GA·13*S*-**3**; (c) GT·13*S*-**3**; (d) GC·13*S*-**3**.

Table 1. Average Nonbonding Distance of 5′G N7−C_{15} and the Angle for N7−C_{15}−O_3 for the Complexes of d(ATGNTA/TAMCAT) with 13*S*-3[a]

GN/MC	5′G N7−C_{15} (Å)[b]	N7−C_{15}−O_3 (deg)[b]
GG/CC	3.49 (0.42)	134.30 (8.7)
GA/TC	3.35 (0.30)	137.19 (8.0)
GT/AC	3.35 (0.33)	139.91 (8.5)
GC/GC	3.44 (0.36)	137.35 (7.9)

[a] The average nonbonding distance of 5′ G N7−C_{15} and the angle of N7−C_{15}−O_3 were obtained for 100 structures being sampled during MD simulations of the complexes of d(ATGNTA/TAMCAT) with 13*S*-**3**. [b] The value in parentheses is the standard deviation.

experimentally observed G alkylation susceptibility. The relative alkylation reactivity of the Gs of the GN sequences as compared with GG [$\ln(I_{G*G}/I_{G*N})$] obtained by the normalized relative G band intensity of Figure 1 is well correlated with the calculated energy difference between GN and GG ($\Delta\Delta E_{GN-GG}$) (Figure 5). It is particularly noteworthy that the component molecules for GG·13*S*-**3** and for GC·13*S*-**3** complexes are the same (i.e., two guanines and two cytocines, and one 13*S*-**3** molecule), but there was a large difference in both calculated ΔE values and the experimentally observed G alkylation susceptibility. On the basis of these results, it is strongly suggested that highly selective 5′ G alkylation by **2** and 13*S*-**3** is due to their preferential intercalation into the GG step. Stacking interaction of the intercalator with both 5′ and 3′ side Gs is the basis for such complex stabilization. It is well-known that the G base is the highest in HOMO energy among nucleobases.[22] Therefore, it is conceivable that the HOMO−LUMO interaction between the HOMO of 3′ G at the intercalation site and the LUMO of the intercalator may play a significant role for the highly selective intercalation into the GG step.

Experimental Section

^{1}H NMR spectra were measured with Varian Mercury 400 (400 MHz) or JEOL JNM α-400 (400 MHz) spectrometers. ^{13}C NMR spectra were measured with a Varian Mercury 400 (100

(22) (a) Sugiyama, H.; Saito, I. *J. Am. Chem. Soc.* **1996**, *118*, 7063−7068. (b) Prat, F.; Houk, K. N.; Foote, C. S. *J. Am. Chem. Soc.* **1998**, *120*, 845−846. (c) Sponer, J.; Leszczynski, J.; Hobza, P. *J. Phys. Chem.* **1996**, *100*, 5590−5596.

Table 2. Calculated Energies of GN·13*S*-**3** at the B3LYP/6-31G(d) Level

run[a]	$E_{GA\cdot 13S\text{-}3}$[b]	$E_{GC\cdot 13S\text{-}3}$[b]	$E_{GG\cdot 13S\text{-}3}$[b]	$E_{GT\cdot 13S\text{-}3}$[b]
1	−3129.111 356 05	−3145.148 432 00	−3145.160 633 82	−3129.105 785 79
11	−3129.111 989 00	−3145.147 885 82	−3145.160 620 22	−3129.105 751 21
21	−3129.110 893 34	−3145.146 527 62	−3145.160 854 67	−3129.109 294 66
31	−3129.109 069 01	−3145.145 856 46	−3145.160 184 99	−3129.110 436 63
41	−3129.109 432 35	−3145.146 633 84	−3145.161 372 33	−3129.110 801 80
51	−3129.112 687 10	−3145.148 324 42	−3145.159 341 72	−3129.111 097 29
61	−3129.109 790 01	−3145.150 900 95	−3145.161 530 37	−3129.110 155 55
71	−3129.109 719 15	−3145.152 326 85	−3145.162 733 91	−3129.109 262 37
81	−3129.109 674 12	−3145.150 200 44	−3145.163 784 51	−3129.107 808 03
91	−3129.109 312 98	−3145.150 255 16	−3145.160 784 61	−3129.106 036 33
av	−3129.110 392 31	−3145.148 734 36	−3145.161 184 12	−3129.108 642 97

[a] Run number corresponds to the structure number of GN·13*S*-**3** complex being sampled during MD simulations. [b] Energy is reported in hartree.

Table 3. Relative Energy Difference of the Intercalation of 13*S*-**3** into the GN/MC and GG/CC Steps[a]

N	E_{GN}[b]	$E_{GN\cdot 13S\text{-}3}$[b,c]	ΔE_{GN}[d,e] (kcal/mol)	$\Delta\Delta E_{GN-GG}$[f] (kcal/mol)
G	−2032.26467	−3145.16118	−5.53 (0.80)	0.00
A	−2016.22521	−3129.11039	1.58 (0.79)	7.11
T	−2016.22932	−3129.10864	5.26 (1.34)	10.79
C	−2032.27840	−3145.14873	10.89 (1.33)	16.43

[a] Energy calculations of GN, 13*S*-**3**, and GN·13*S*-**3** complex were carried out at the DFT-HF hybrid B3LYP/6-31G(d) level. [b] Energies (*E*) are reported in hartree. [c] An average energy of GN·13*S*-**3** was obtained from Table 2. [d] $\Delta E_{GN} = E_{GN\cdot 13S-3} - E_{GN} - E_{13S-3}$, where E_{13S-3} was −1112.887 70 hartree. [e] The value in parentheses is the standard deviation. [f] $\Delta\Delta E_{GN-GG} = \Delta E_{GN} - \Delta E_{GG}$.

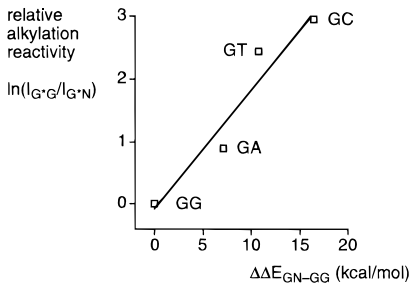

Figure 5. Calculated $\Delta\Delta E_{GN-GG}$ vs relative alkylation reactivity [ln(I_{G*G}/I_{G*N})] experimentally obtained. Correlation coefficient $r = 0.966$.

MHz) spectrometer. Coupling constants (*J* values) are represented in hertz. The chemical shifts are expressed in ppm downfield from tetramethylsilane, using residual solvent as an internal standard. IR spectra were recorded on a Jasco FT-IR-5M spectrophotometer. Mass spectra were recorded on a JEOL JMS DX-300 or a JEOL JMS SX-102A spectrometer. Sequence gel electrophoresis was carried out on a Gibco BRL model S2 apparatus. Densitometric analysis of the gel was carried out using a Bio-Rad GS-700 imaging densitometer with analytical software Molecular Analyst (version 2.1). Wakogel C-200 was used for silica gel flash chromatography. Precoated TLC plates Merck silica gel 60 F_{254} were used for monitoring reactions and also for preparative TLC. Gel permeation chromatography (GPC) was carried out on JAI LC-908 using a polystyrene column. Ether and tetrahydrofuran (THF) were distilled under N_2 from sodium/benzophenone ketyl prior to use. All enzymes used in these studies were from commercial sources. [γ-^{32}P]-ATP (6000 Ci/mmol) was obtained from Amersham.

(2*R*,3*R*)-1-(4-Methoxybenzyloxy)-3-methyl-4-pentyne-2,3-diol (5). To a suspension of sodium hydride (60%, 4.50 g, 113 mmol) in *N*,*N*-dimethylformamide (10 mL) was added (*E*)-3-methylpent-2-en-4-yn-1-ol (10.01 g, 104 mmol) at 0 °C, and the reaction mixture was stirred for 10 min. To this mixture was added *p*-methoxybenzyl chloride (15.5 mL, 114.3 mmol) at 0 °C, and the mixture was stirred for 30 min. The resulting mixture was diluted with saturated NH_4Cl and extracted with ethyl acetate. The crude product was purified by column chromatography on silica gel, eluting with 5% ethyl acetate in hexane to give (*E*)-1-(4-methoxybenzyloxy)-3-methyl-2-penten-4-yne (**4**) (20.6 g, 102 mmol, 98%) as a yellow oil: ^{1}H NMR (400 MHz, $CDCl_3$) δ 7.24 (d, 2H, $J = 8.8$ Hz), 6.86 (d, 2H, $J = 8.7$ Hz), 6.07 (m, 1H), 4.42 (s, 2H), 4.05 (dt, 2H, $J = 0.7$, 6.6 Hz), 3.79 (s, 3H), 2.81 (s, 1H), 1.78 (s, 1H); IR ($CHCl_3$) 3304, 3021, 3009, 1612, 1513, 1249, 1217, 1173, 1035, 773, 769 cm^{-1}. A mixture of AD-mix-β (12.0 g) and methanesulfonamide (0.82 g, 8.62 mmol) in *tert*-butyl alcohol (40 mL) and H_2O (40 mL) was stirred at 0 °C for 30 min. To the mixture was added **4** (1.73 g, 8.54 mmol) at 0 °C, and the whole mixture was stirred for 2 days. The reaction was quenched by adding Na_2SO_3 (15 g) followed by stirring for 2 h. The resulting mixture was extracted with ethyl acetate, and the combined organic layer was washed with 1 N NaOH. The crude product was purified by column chromatography on silica gel, eluting with 20−100% ethyl acetate in hexane to give **5** (1.63 g, 76%) as a colorless oil: ^{1}H NMR (400 MHz, $CDCl_3$) δ 7.24 (d, 2H, $J = 8.7$ Hz), 6.86 (d, 2H, $J = 8.7$ Hz), 4.49 and 4.48 (d × 2, each 1H, $J = 11.4$ Hz), 3.79 (s, 3H), 3.77 (m, 1H), 3.72 (dd, 1H, $J = 4.7$, 9.2 Hz), 3.59 (dd, 1H, $J = 6.3$, 9.2 Hz), 3.26 (s, 1H), 2.53 (d, 1H, $J = 5.0$ Hz), 2.46 (s, 1H), 1.47 (s, 3H); ^{13}C NMR (100 MHz, $CDCl_3$) δ 159.06, 129.28, 129.26, 113.69, 85.28, 74.71, 73.16, 72.73, 70.56, 69.77, 55.20, 25.41; IR ($CHCl_3$) 3562, 3306, 3011, 2937, 1514, 1250, 1174, 1087, 1036, 734 cm^{-1}; MS (EI) *m*/*z* (%) 250 (M^+) (21), 137 (100), 121 (100); HRMS (EI) calcd for $C_{14}H_8O_4$ (M^+), 250.1204; found, 250.1201.

(4*R*,5*R*)-4-Ethynyl-5-(4-methoxybenzyloxymethyl)-2,2,4-trimethyl-1,3,-dioxolane (6). To a solution of **5** (1.97 g, 7.87 mmol), 2,2-dimethoxypropane (4.9 mL, 39.9 mmol), and anhydrous $CuSO_4$ (6.29 g, 39.4 mmol) in acetone (50 mL) was added *dl*-camphorsulfonic acid (92.4 mg, 0.40 mmol) at 0 °C, and the mixture was stirred for 3 h. The resulting mixture was filtered, diluted with saturated $NaHCO_3$, concentrated in vacuo to remove acetone, and extracted with ethyl acetate. The crude product was purified by column chromatography on silica gel, eluting with 15% ethyl acetate in hexane to give **6** (2.17 g, 95%) as a colorless oil: ^{1}H NMR (400 MHz, $CDCl_3$) δ 7.26 (d, 2H, $J = 8.8$ Hz), 6.86 (d, 2H, $J = 8.7$ Hz), 4.58 (d, 1H, $J = 11.7$ Hz), 4.46 (d, 1 H, $J = 11.7$ Hz), 4.42 (dd, 1H, $J = 5.0$, 6.5 Hz), 3.79 (s, 3H), 3.555 (d, 1H, $J = 5.0$ Hz), 3.551 (d, 1H, $J = 6.4$ Hz), 2.48 (s, 1H), 1.46 (d, 3H, $J = 0.5$ Hz), 1.42 (d, 3H, $J = 0.5$ Hz), 1.34 (s, 3H); ^{13}C NMR (100 MHz, $CDCl_3$) δ 158.92, 129,50, 129,10, 113.54, 109.34, 85.17, 81.44, 74.26, 73.02,

72.29, 67.79, 55.10, 28.15, 25.70, 23.18; IR ($CHCl_3$) 3020, 2993, 1513, 1375, 1249, 1088, 780 cm^{-1}; MS (EI) *m*/*z* (%) 290 (M^+) (13), 275 (47), 232 (81), 137 (97), 121 (100); HRMS (EI) calcd for $C_{17}H_{22}O_4$ (M^+), 290.1518; found, 290.1524.

(4*R*,5*R*)-5-(4-Methoxybenzyloxymethyl)-2,2,4-trimethyl-4-(2-trimethylsilylethynyl)-1,3-dioxolane (7). To a solution of **6** (1.63 g, 5.62 mmol) in THF (20 mL) was added lithium hexamethyldisilazide (LHMDS) (1.0 M solution in THF, 6.2 mL, 6.20 mmol) at −78 °C, and the mixture was stirred for 10 min. To the mixture was added trimethylchlorosilane (0.78 mL, 6.16 mmol) at −78 °C, and the reaction mixture was warmed to 0 °C and stirred for another 20 min. The resulting mixture was diluted with saturated NH_4Cl and extracted with ethyl acetate. The crude product was purified by column chromatography on silica gel, eluting with 15% ethyl acetate in hexane to give **7** (1.79 g, 88%) as a colorless oil: ^{1}H NMR (400 MHz, $CDCl_3$) δ 7.27 (d, 2H, J = 8.8 Hz), 6.86 (d, 2H, J = 8.7 Hz), 4.58 (d, 1H, J = 11.6 Hz), 4.46 (d, 1H, J = 11.6 Hz), 4.39 (dd, 1H, J = 4.4, 7.0 Hz), 3.79 (s, 3H), 3.57 (dd, 1H, J = 4.4, 10.3 Hz), 3.52 (dd, 1H, J = 7.0, 10.3 Hz), 1.46 (s, 3H), 1.41 (s, 3H), 1.32 (s, 3H), 0.13 (s, 9H); ^{13}C NMR (100 MHz, $CDCl_3$) δ 159,00, 129.75, 129.14, 113.65, 109.37, 106.72, 88.55, 81.76, 74.84, 73.05, 68.13, 55.25, 28.33, 25.89, 23.35, −0.04; IR ($CHCl_3$) 3020, 1513, 1250, 1180, 1087, 848 cm^{-1}; MS (FAB) *m*/*z* (%) 362 (M^+) (5), 347 [$(M - Me)^+$] (10), 303 (17), 121 (100); HRMS (FAB) calcd for $C_{20}H_{30}O_4Si$ (M^+), 362.1913; found, 362.1896.

(4*R*,5*R*)-5-(Hydroxymethyl)-2,2,4-trimethyl-4-(2-trimethylsilylethynyl)-1,3,-dioxolane (8). To a solution of **7** (0.31 g, 0.85 mmol) in dichloromethane (18 mL) and H_2O (1 mL) was added DDQ (0.23 g, 1.01 mmol) at 0 °C, and the mixture was stirred at ambient temperature for 4 h. The resulting mixture was diluted with saturated $NaHCO_3$, and extracted with ethyl acetate. The crude product was purified by column chromatography on silica gel, eluting with 60% toluene in hexane to give **8** (0.18 g, 99%) as colorless needles. Recrystallization from 5% benzene in hexane at −30 °C provided optically pure **8**: mp 45 °C; $[\alpha]_D^{25}$ = +19.34 (*c* 0.610, MeOH); ^{1}H NMR (400 MHz, $CDCl_3$) δ 4.31 (dd, 1H, J = 3.9, 7.4 Hz), 3.73 (2H), 1.73 (m, 1H), 1.49 (s, 3H), 1.43 (s, 3H), 1.37 (s, 3H), 0.14 (s, 9H); ^{13}C NMR (100 MHz, $CDCl_3$) δ 109.48, 106.77, 88.86, 83.38, 74.72, 61.32, 28.39, 25.95, 23.43, −0.05; IR ($CHCl_3$) 3020, 1217, 847, 754 cm^{-1}; MS (EI) *m*/*z* (%) 227 [$(M - Me)^+$] (82), 209 (35), 182 (35), 167 (100), 155 (70), 124 (88); HRMS (EI) calcd for $C_{11}H_{19}O_3Si$ [$(M - Me)^+$], 227.1103; found, 227.1098. Anal. Calcd for $C_{12}H_{22}O_3Si$: C, 59.46; H, 9.15. Found: C, 59.20; H, 9.30.

To the solution of alcohol (4*S*,5*S*)-**8** (196 mg, 0.92 mmol) in dichloromethane (5 mL) were added (−)-(*S*)-MTPA acid (215 mg, 0.92 mmol), DCC (191 mg, 0.92 mmol), and DMAP (12.0 mg, 0.098 mmol) at ambient temperature, and the mixture was stirred at ambient temperature for 1 h. The mixture was diluted with ethyl acetate, filtered, and concentrated in vacuo. The crude product was purified by column chromatography on silica gel, eluting with toluene to give a diastereomeric mixture of MTPA ester **15** (354 mg). The mixture was separated by HPLC on Daicel Chiralcel OJ (10 × 250 mm, elution with 2% hexane in 2-propanol at a flow rate of 1.0 mL/min). The major fraction was collected and concentrated in vacuo to give pure **15**: ^{1}H NMR ($CDCl_3$, 400 MHz,) δ 7.55−7.53 (2 H), 7.42−7.37 (3 H), 4.47−4.37 (3 H), 3.55 (d, 3 H, J = 1.1 Hz), 1.44 (s, 3 H), 1.40 (s, 3 H), 1.36 (s, 3 H), 0.13 (s, 3 H). To the solution of **15** (101 mg, 0.22 mmol) in dichloromethane (2 mL) was added DIBAL (1.0 M in toluene, 0.5 mL, 0.5 mmol) at −78 °C, and the mixture was stirred at −78 °C for 15 min and at 0 °C for 15 min. The resulting mixture was diluted with methanol (10 mL), stirred at ambient temperature for 10 min, further diluted with 5 mL each of ethyl acetate and saturated Rochelle salt, and stirred at ambient temperature for 30 min. The mixture was extracted with ethyl acetate. The crude product was purified by column chromatography on silica gel, eluting with 30% ethyl acetate in hexane to give optically pure (4*S*,5*S*)-**8** (41.0 mg, 0.19 mmol): $[\alpha]_D^{25}$ = −19.17 (*c* 0.120, MeOH).

(4*R*,5*R*,*Z*)-5-Propenyl-2,2,4-trimethyl-4-(trimethylsilylethynyl)-1,3,-dioxolane (9). To a solution of **8** (0.81 g, 3.34 mmol) in dichloromethane (30 mL) was added Dess−Martin periodinane (1.7 g, 4.01 mmol) at ambient temperature, and the mixture was stirred at that temperature for 1 h. The resulting mixture was diluted with saturated $Na_2S_2O_3$ and saturated $NaHCO_3$ and then extracted with ethyl acetate. The crude product was purified by column chromatography on silica gel, eluting with 25% ethyl acetate in hexane to give (4*R*,5*S*)-5-formyl-2,2,4-trimethyl-4-(2′-trimethylsilylethynyl)-1,3,-dioxolane (0.76 g, 94%) as a colorless oil: ^{1}H NMR ($CDCl_3$, 400 MHz) δ 9.61 (d, 2 H, J = 2.2 Hz), 4.54 (d, 2 H, J = 2.4 Hz), 1.56 (d, 3 H, J = 0.5 Hz), 1.53 (d, 3 H, J = 0.5 Hz), 1.43 (s, 3 H), 0.16 (s, 9 H); MS (EI) *m*/*e* (%) 235[$(M - Me)^+$], (10), 153 (55), 100 (74), 85 (100). To a solution of aldehyde (0.67 g, 2.80 mmol) in toluene (20 mL) was added a toluene solution of ethylidentriphenylphosphorane, which was prepared from ethyltriphenylphosphonium bromide (1.86 g, 5.01 mmol) and potassium hexamethyldisilazide (10.0 mL, 0.5 M in toluene, 5.0 mmol) in toluene (10 mL) under refluxing for 2 h, at −78 °C, and the mixture was stirred 1 h at that temperature and then for another 1 h at 0 °C. The resulting mixture was diluted with saturated NH_4Cl and extracted with ethyl acetate. The crude product was purified by column chromatography on silica gel, eluting with 30% toluene in hexane to give **9** (0.55 g, 78%, *Z*/*E* = 10:1 mixture) as a colorless oil. Pure *Z*-isomer for analysis could be isolated by recycling preparative HPLC: ^{1}H NMR (400 MHz, $CDCl_3$) δ 5.82 (ddq, 1H, J = 1.3, 7.0, 11.1 Hz), 5.40 (m, 1H), 5.05 (d, 1H, J = 8.5 Hz), 1.78 (dd, 3H, J = 1.8, 7.0 Hz), 1.47 (s, 3H), 1.43 (s, 3H), 1.30 (s, 3H), 0.13 (s, 9H); ^{13}C NMR (100 MHz, $CDCl_3$) δ 130.47, 124.65, 108.85, 106.99, 88.58, 78.96, 76.13, 28.32, 25.95, 24.20, 14.09, −0.09; IR ($CHCl_3$) 3017, 1730, 1250, 723 cm^{-1}; MS (EI) *m*/*z* (%) 237 [$(M - Me)^+$] (11), 195 (21), 182 (28), 167 (38), 97 (100); HRMS (EI) calcd for $C_8H_{21}O_2Si$ [$(M - Me)^+$], 237.1311; found, 237.1322.

(4*R*,5*R*,*Z*)-4-Ethynyl-5-propenyl-2,2,4-trimethyl-1,3-dioxolane (10). To a solution of **9** (105.1 mg, 0.42 mmol) in methanol (1 mL) was added a catalytic amount of sodium methoxide at 0 °C, and the mixture was stirred at ambient temperature for 4 h. The resulting mixture was diluted with saturated NH_4Cl and extracted with ether. Concentration of the organic layer afforded **10** (51.6 mg, 69%) as a colorless oil: ^{1}H NMR (400 MHz, $CDCl_3$) δ 5.84 (ddq, 1H, J = 1.2, 7.0, 11.1 Hz), 5.40 (ddq, 1H, J = 1.8, 8.6, 11.1 Hz), 5.08 (dd, 1H, J = 1.1, 8.6 Hz), 2.47 (s, 1H), 1.78 (dd, 3H, J = 1.8, 7.0 Hz), 1.48 (s, 3H), 1.44 (s, 3H), 1.34 (s, 3H); ^{13}C NMR (100 MHz, $CDCl_3$) δ 130.98, 124.27, 109.02, 85.47, 78.68, 75.66, 72.33, 28.32, 25.91, 24.23, 14.03; IR ($CHCl_3$) 3017, 2932, 1721, 1291, 1222, 1077, 788 cm^{-1}; MS (EI) *m*/*z* (%) 165 [$(M - Me)^+$] (100), 149 (13), 110 (80), 97 (60); HRMS (EI) calcd for $C_{10}H_{13}O_2$ [$(M - Me)^+$], 165.0915; found, 165.0920.

(4*R*,5*R*,*Z*)-4-[3-[1-(*tert*-Butyldimethylsilyloxy)-2-anthryl]-3-hydroxy-1-propynyl]-5-(1-propenyl)-2,2,4-trimethyl-1,3-dioxorane (12). To a solution of **10** (99.2 mg, 0.55 mmol) and anhydrous $CeCl_3$ (411 mg, 1.7 mmol) in THF (5 mL) stirred at

ambient temperature for 10 min was added LHMDS (1.1 mL, 1.0 M in THF, 1.1 mmol) at −78 °C, and the mixture was stirred at −78 °C for 15 min. A solution of **11** (187 mg, 0.55 mmol) in THF (1 mL) was added to the mixture at −78 °C, and the whole mixture was stirred at −78 °C for 15 min. The reaction was quenched by adding saturated NH_4Cl at −78 °C, and the resulting mixture was extracted with ethyl acetate. The crude product was purified by column chromatography on silica gel, eluting with 35% toluene in hexane to give a mixture of diastereoisomer of **12** (98.8 mg, 35%) as a yellow oil: ^{1}H NMR (400 MHz, $CDCl_3$) δ 8.67 (s, 1H), 8.34 (s, 1H), 7.99, 7.96 (s × 2, total 2H), 7.73−7.63 (2H), 7.50−7.43 (2H), 6.06−6.04 (1H), 5.83−5.75 (1H), 5.42−5.36 (1H), 5.07, 5.03 (dd × 2, total 1H, J = 1.1, 8.6 Hz,), 2.16−2.12 (1H), 1.70, 1.60 (dd × 2, total 3H, J = 1.7, 7.0 Hz), 1.48−1.43 (6H), 1.37, 1.35 (s × 2, total 3H), 1.20, 1.19 (s × 2, total 9H), 0.24−0.22 (6H); IR ($CHCl_3$) 3571, 3019, 1216 cm^{-1}; MS (EI) *m*/*e* (%) 516 (M^+) (2), 222 (70), 75 (100).

(4*S*,5*R*,*Z*)-4-(4*H*-Anthra[1,2-*b*]pyran-2-yl)-5-(1-propenyl)-2,2,4-trimethyl-1,3-dioxorane (13). To a solution of **12** (56.1 mg, 109 μmol) in dichloromethane (3 mL) was added manganese(IV) oxide (50 mg), and the reaction mixture was stirred for 3 h at ambient temperature. The mixture was diluted with ethyl ether, filtered, and concentrated in vacuo. The crude product was purified by column chromatography on silica gel, eluting with 13% ethyl acetate in hexane to give (4*R*,5*R*,*Z*)-4-[3-[1-(*tert*-butyldimethylsilyloxy)-2-anthryl]-3-oxo-1-propynyl]-5-propenyl-2,2,4-trimethyl-1,3-dioxorane (38.7 mg, 75.2 μmol, 69%) as a yellow oil: MS (EI) *m*/*e* (%) 457 [(M − *t*-Bu)$^+$] (10), 368 (18), 294 (37), 149 (100); HRMS (EI) calcd for $C_{32}H_{38}O_4Si$ [(M − *t*-Bu)$^+$], 457.1836; found, 457.1840. This ketone was used immediately for the next reaction. To a solution of ketone (29.8 mg, 57.9 μmol) and 18-crown-6 (30.7 mg, 116 μmol) in *N*,*N*-dimethylformamide (3 mL) was added a potassium fluoride (6.8 mg, 117 μmol) at 0 °C, and the mixture was stirred at ambient temperature for 1 h. The resulting mixture was diluted with saturated NH_4Cl and extracted with ethyl acetate. The crude product was purified by column chromatography on silica gel, eluting with 13% ethyl acetate in hexane to give **13** (17.3 mg, 43.2 μmol, 75%) as a yellow oil: ^{1}H NMR (400 MHz, $CDCl_3$) δ 8.84 (s, 1H), 8.46 (s, 1H), 8.08−8.04 (3H), 7.87 (d, 1H, J = 9.0 Hz), 7.63−7.56 (2H), 6.85 (s, 1H), 6.12−6.04 (m, 1H), 5.85−5.78 (m, 1H), 5.10 (d, 1H, J = 10.0 Hz), 1.68 (s, 3H), 1.63 (s, 3H), 1.56 (s, 3H), 1.43 (dd, 3H, J = 7.0, 1.8 Hz); IR ($CHCl_3$) 3263, 2995, 1650, 1386, 1105 cm^{-1}; MS (EI) *m*/*e* (%) 400 (M^+) (59), 289 (100), 288 (75), 149 (43); HRMS (EI) calcd for $C_{26}H_{24}O_4$ (M^+), 400.1674; found, 400.1658.

(2*S*,3*R*,4*Z*)-2-(4*H*-Anthra[1,2-*b*]pyran-2-yl)-4-hexene-2,3-diol (14). To a solution of **13** (14.4 mg, 36.0 μmol) in THF (1 mL) and AcOH (1 mL) was added 0.2 M HCl (0.1 mL) at 0 °C, and the mixture was stirred at ambient temperature for 3 days. The resulting mixture was poured into saturated $NaHCO_3$ and extracted with ethyl acetate. The crude product was purified by column chromatography on silica gel, eluting with 50% ethyl acetate in hexane to give **14** (11.8 mg, 32.7 μmol, 91%) as a white solid: ^{1}H NMR (400 MHz, $CDCl_3$) δ 8.92 (s, 1H), 8.39 (s, 1H), 8.12−8.04 (2H), 7.90 (d, 1H, J = 9.0 Hz), 7.72 (d, 1H, J = 9.0 Hz), 7.64−7.57 (2H), 6.82 (s, 1H), 5.93−5.85 (m, 1H), 5.74−5.67 (m, 1H), 5.13 (d, 1H, J = 9.3 Hz), 3.34 (br, 1H), 2.53 (br, 1H), 1.80 (dd, 3H, J = 1.8, 7.0 Hz), 1.64 (s, 3H); MS (FAB) (NBA) *m*/*e* 361 [(M + H)$^+$]; HRMS (FAB) calcd for $C_{23}H_{21}O_4$ [(M + H)$^+$], 361.1440; found, 361.1446.

(2*S*,3*R*,4*Z*)-2-(4*H*-Anthra[1,2-*b*]pyran-2-yl)-2,3-epoxy-4-hexene (13*S*-3). To a solution of **14** (6.9 mg, 19.1 μmol) and triphenylphosphine (7.0 mg, 26.7 μmol) in toluene (1 mL) was added DEAD (6 μL, 37.9 μmol) at 0 °C, and the mixture was stirred at ambient temperature for 24 h. The resulting mixture was concentrated in vacuo and purified by column chromatography on silica gel, eluting with 13% toluene in hexane to give 13*S*-**3** (4.1 mg, 63%) as a white solid: ^{1}H NMR (400 MHz, $CDCl_3$) δ 9.00 (s, 1H), 8.47 (s, 1H), 8.14 (m, 1H), 8.08−8.04 (2H), 7.88 (d, 1H, J = 9.0 Hz), 7.63−7.56 (2H), 6.61 (s, 1H), 5.81 (ddd, 1H, J = 1.1,7.1, 11.2 Hz), 5.18 (dq, 1H, J = 1.7, 8.6 Hz), 3.95 (d, 1H, J = 8.6 Hz), 1.96 (s, 3H), 1.85 (dd, 3H, J = 1.7, 7.1 Hz); IR ($CHCl_3$) 3129, 1651, 1223, 909 cm^{-1}; MS (EI) *m*/*e* (%) 342 (M^+) (100), 300 (33), 220 (76); HRMS (EI) calcd for $C_{23}H_{18}O_3$ (M^+), 342.1256; found, 342.1245.

Cleavage of ^{32}P 5′-End-Labeled Oligodeoxynucleotide by 13*S*-3 and 13*R*-3. Single-stranded 43-mer DNA oligomer 5′-d(TTTTTGTTTGTTAGTTCGTTTGCTTGGTTGATTGTTT-GTTTTT)-3′ (400 pmol), purchased from Greiner Japan Co. Ltd., was 5′-end-labeled by phosphorylation with [γ-^{32}P]ATP (4 μL) (Amersham, 370 MBq/μL) and T4 polynucleotide kinase (4 μL) (Takara, 10 units/μL) using standard procedures. The 5′ end-labeled DNA was recovered by ethanol precipitation, further purified by 15% nondenatured gel electrophoresis, and isolated by a crush and soak method. The isolated DNA was incubated with equimolar of the complementary strand in 100 μL of water at 90 °C for 5 min and cooled slowly to ambient temperature for duplex formation. 13*S*-**3** and 13*R*-**3** (50 μL) was incubated with 10 μL of calf thymus DNA and ∼1.0 × 10^6 cpm ^{32}P 5′-end-labeled ODN duplex in 20 mM Tris-HCl buffer (100 μL, pH 7.6) at 37 °C. After a certain time interval, an aliquot of the sample (10 μL) was separated from the reaction mixture and precipitated with methanol. The recovered DNA was dissolved in 100 μL of 10% (v/v) piperidine and heated at 90 °C for 30 min. The mixture was concentrated in vacuo and resuspended in 10 μL of 80% formamide loading buffer (80% formamide, 1 mM EDTA, 0.1% xylene cyanole, and 0.1% bromophenol blue). The samples (1 μL) were loaded onto 15% polyacrylamide and 7 M urea sequence gel and electrophoresed at 1900 V for ∼2 h. The gel was dried, exposed to X-ray film with intensifying sheet at −70 °C, and analyzed by densitometer.

Supercoiled DNA-Unwinding Assay. To a solution of pBR322 plasmid DNA (250 ng, Nippon Gene) in topo I reaction buffer (10 mM Tris-HCl, pH 7.9, 1 mM EDTA, 150 mM NaCl, 0.1 mM spermidine, 5% glycerol, 0.1% BSA) was added human topoisomerase I (TopoGEN, 4 units). The reaction mixture was incubated for 30 min at 37 °C. Drugs **16**, **17**, and **18** (100 μM) were added, and incubation was continued for another 30 min at 37 °C. The reaction was terminated by addition of SDS to 1%. After proteinase K was added to 50 μg/mL, the mixture was digested for 20 min at 56 °C. Addition of 0.1 volume of 10× gel loading buffer was followed by chloroform extraction. Different forms of DNA were separated at room temperature on a 1% agarose gel. The gel was stained for 30 min with ethidium bromide (0.5 μM/mL) and destained for 20 min in water. It was placed on a UV transilluminator (313 nm) and photographed with Polaroid 665 film.

Acknowledgment. We thank Prof. S. Rychnovsky (University of California, Irvine) for many helpful discussions. We are grateful to the JST supercomputer complex for allocation of supercomputer time. This research was in part supported by a Grant-in-Aid for Priority Research from the Ministry of Education, Science, Sports and Culture.

JA980801Q